**Showcasing research from the Inorganic Synthetic Laboratory, Department of Applied Chemistry and Kagami Memorial Research Institute for Materials Science and Technology, Waseda University, Tokyo, Japan.**

Fabrication of colloidal crystals composed of pore-expanded mesoporous silica nanoparticles prepared by a controlled growth method

Colloidal crystals composed of pore-expanded MSNs have been prepared using a sophisticated particle growth method to control the pore size of colloidal MSNs while retaining their high monodispersity enough to form colloidal crystals. By adding triisopropylbenzene (TIPB) only during the growth process with the stepwise addition of tetrapropoxysilane (TPOS), the particle size can be tuned from 60 nm to 100 nm, while the pore size can be tuned from 3 nm to more than 10 nm which is the largest size among previous MSNs capable of forming colloidal crystals.
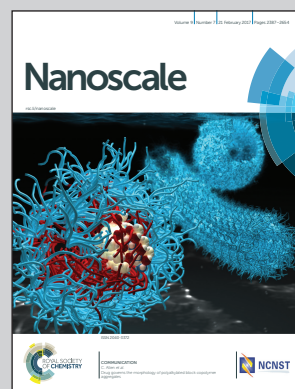
ROYAL SOCIETY OF CHEMISTRY

rsc.li/nanoscale

Nanoscale

Fabrication of colloidal crystals composed of pore-expanded mesoporous silica nanoparticles prepared by a controlled growth method†

Eisuke Yamamoto,[a] Seiya Mori,[a] Atsushi Shimojima,[a] Hiroaki Wada[a] and Kazuyuki Kuroda*[a,b]

Colloidal crystals composed of mesoporous silica nanoparticles (MSNs) are expected to have various applications because of their unique hierarchical structures and tunable functions. The expansion of the mesopore size is important for introducing guest species which cannot be accommodated by using conventional colloidal crystals of MSNs; however, the preparation of MSNs with a controllable pore size, suitable for the fabrication of colloidal crystals, still remains a challenge. In this study, we fabricated colloidal crystals composed of pore-expanded MSNs using a sophisticated particle growth method to control the pore size of colloidal MSNs while retaining their monodispersity high enough to form colloidal crystals. By adding triisopropylbenzene (TIPB) only during the growth process with the stepwise addition of tetrapropoxysilane (TPOS), the particle size can be tuned from 60 nm to 100 nm, while the pore size can be tuned from 3 nm to ten plus several nm which is the largest size among the previous MSNs capable of forming colloidal crystals. These novel colloidal crystals should contribute to the expansion of nanomaterials science.

[a]Department of Applied Chemistry, Faculty of Science and Engineering, Waseda University, Ohkubo 3-4-1, Shinjuku-ku, Tokyo, 169-8555, Japan. E-mail: kuroda@waseda.jp
[b]Kagami Memorial Research Institute for Materials Science and Technology, Waseda University, Nishiwaseda 2-8-26, Shinjuku-ku, Tokyo, 169-0051, Japan
†Electronic supplementary information (ESI) available. See DOI: 10.1039/c6nr07416b

Introduction

Colloidal crystals have attracted great attention for numerous applications, such as templates[1–10] and photonic crystals[11–13] because of ordered interparticle pores and the three-dimensional periodic change of their refractive indices. Colloidal crystals are generally prepared through the self-assembly of monodisperse colloidal nanoparticles; it is essential for their applications to control various factors of the component nanoparticles, including their size, morphology, structure, composition, and porosity. Among these factors, the porosity of the nanoparticles is highly important because it strongly affects their refractive indices and the accessibility of guest species.[14–17] Guest species introduced in colloidal crystals (or their inverse materials) have anomalous features generated by the special features of colloidal crystals, such as slow photons, which enable us to use the guest species more effectively.[18–20]

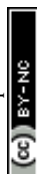Mesoporous silica nanoparticles (MSNs) are the most appropriate material possessing the porosity of nano-

particles.[21] A few groups have succeeded in preparing colloidal crystals composed of MSNs.[22–26] Unlike dense (nonporous) silica nanoparticles, MSNs have desirable features in their applicability as colloidal crystals.[17] Colloidal crystals composed of MSNs can be used as unique vessels to accommodate various additives in the mesopores[27–31] to create cutting-edge materials. For example, colloidal crystals composed of quartz were prepared by introducing flux in the mesopores to enable the crystallization of amorphous silica into α-quartz.[32] MSNs are also useful for producing unique photonic crystals.[23,26,33,34] The mesopores allow the introduction of a large amount of guest species into the photonic crystals. This feature enables these crystals to be used as gas sensors and photonic lasers.[23,34–36] Interestingly, the introduction of functional substances solely into the mesopores of the component nanoparticles enables the functionalization of the photonic crystals without widening the photonic band gap. In fact, a notable modification of the Faraday rotation was observed when Fe_2O_3 nanoparticles were embedded in the mesopores of photonic crystals.[33] The variety and amount of introducible guest species are expected to be extended to a much larger range for further functionalization.

Control of the pore size is essential because it strongly affects the accessibility and the introducible amount of guest species. Furthermore, expansion of the pores enables the introduction of large guest species that cannot be accommodated using conventional colloidal crystals. There are various

kinds of pore expanded MSNs;[37,38] however to the best of our knowledge, only Yano *et al.* have succeeded in fabricating colloidal crystals composed of pore-expanded MSNs with carbon in their mesopores.[30] Unfortunately, the pore size of the component MSNs is smaller than 4.2 nm, and the size of the MSNs is several hundred nanometers. This limited controllability of both the particle size and pore size strongly inhibits the applicability of these MSNs as colloidal crystals. Larger pore sizes are preferable to accommodate functional substances, such as nanorods and biomolecules. Also, the particle size should be much smaller to enable good control of the optical properties and to use them as templates to produce various nanomaterials. It is essential to develop a novel method to fabricate colloidal crystals composed of pore-expanded mesoporous silica nanoparticles with controlled particle sizes.

To prepare colloidal crystals composed of pore-expanded MSNs, the nanoparticles must meet the following requirements: (1) monodispersity (relative standard deviation should be set under 10%) and (2) colloidal stability to enable thermodynamically favourable assemblies. Although the pore size of MSNs is usually controlled by using an appropriate method, it is difficult to obtain MSNs with such high monodispersity, high colloidal stability and controllability of pore sizes. The use of additional agents alters both the hydrolysis and condensation rates of the silica sources, which strongly affects the size distribution of the MSNs.[39] Several groups successfully synthesized monodisperse MSNs with expanded pore sizes;[38,40–48] however, they did not achieve ordered colloidal crystals, except for the report by Yano *et al.*[30] This may be due to insufficient colloidal stability. While there are some reports on the preparation of pore-expanded MSNs with high colloidal stability,[21,39] their monodispersity is not sufficient to form colloidal crystals. The preparation of pore-expanded MSNs suitable for the fabrication of colloidal crystals remains a challenge.

On the other hand, a seed growth method has been applied to obtain MSNs, whose factors like the composition and size are controlled, because this method allows us to prepare MSNs step by step.[49–53] Recently, we reported the successful preparation of colloidal monodisperse MSNs that can form colloidal crystals by preparing precisely size-controlled MSNs, followed by the growth of the seed MSNs by the addition of tetrapropoxysilane.[25] This method enabled us to fabricate colloidal crystals composed of MSNs with various particle sizes. During the course of our study on this topic, we became convinced that our growth method can enable the retention of monodispersity even in the presence of additives, which is one of the core findings of this study. This tolerance toward additives will allow us to use pore-expanding agents without altering the size distribution of the MSNs. Although pore expanded MSNs have been already prepared by a seed growth method, the particle size distribution is broad because of the spontaneous nucleation.[54]

Here, we report the fabrication of colloidal crystals composed of pore-expanded MSNs. The pore-expanded MSNs with extremely high monodispersity and colloidal stability high enough to form colloidal crystals were prepared using a sophisticated controlled growth method in which the pore-expanding agents are added only in the seed growth period (Scheme 1). By changing the amounts of pore-expanding agents added during the growth process, we succeeded in controlling pore sizes while almost entirely retaining the high monodispersity and colloidal stability. Although the fact that the pore expanded MSNs prepared by conventional methods have not formed ordered colloidal crystals may be due to their lack of monodispersity or colloidal stability, the pore-expanded monodisperse colloidal MSNs prepared by using our method successfully formed colloidal crystals.
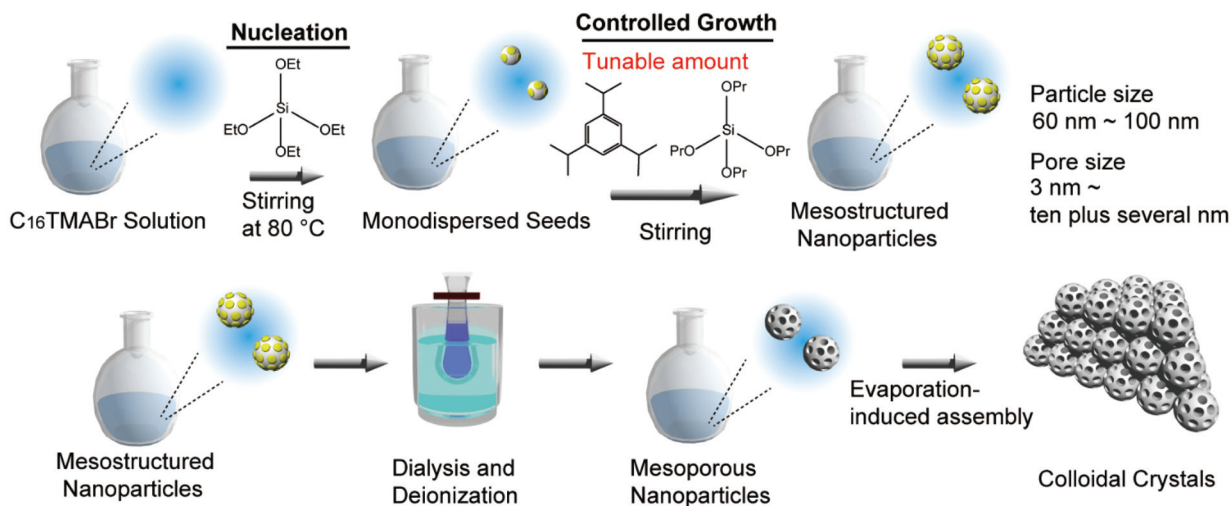
Scheme 1 Schematic illustration of the preparative method of monodisperse mesoporous silica nanoparticles with controlled particle and pore sizes and the fabrication of colloidal crystals.

Experimental

Materials

Hexadecyltrimethylammonium bromide (C_{16}TMABr), tri-ethanolamine (TEA) as a base catalyst and acetic acid were purchased from Wako Pure Chem. Ind., Ltd. 1,3,5-Triisopropylbenzene (TIPB) and tetrapropoxysilane (TPOS: $Si(OC_3H_7)_4$) were purchased from Tokyo Kasei Co., Ltd. Tetraethoxysilane (TEOS: $Si(OC_2H_5)_4$) was purchased from KISHIDA Chemical Co., Ltd. All the compounds were used without further purification. Amberlite MB-1 (Dow Chemical Co.) was used as an amphoteric ion-exchange resin.

Preparation of pore-expanded monodisperse colloidal mesostructured silica nanoparticles

First, the seed nanoparticles were prepared. TEA (0.7 g) and 3.33 g of C_{16}TMABr were dissolved in 400 mL of deionized water in a round-bottomed flask (500 mL). The mixture was stirred for 1 h at 80 °C using a magnetic stirrer with a football-type stirring bar. Then, 0.78 mL of TEOS was added to the solution with stirring at 900 rpm and the mixture was reacted at 80 °C for 1 h. The obtained colloidal solution was slowly cooled to room temperature with stirring. This sample is denoted as TIPB-0-seed.

Second, the seed nanoparticles were grown by the seed-growth method. A pore-expanding agent, TIPB (0.109 mL, 0.272 mL or 0.544 mL) was added to a colloidal solution of TIPB-0-seed (50 mL) in a round-bottomed flask. Then, 0.29 mL of TPOS was added. The colloidal solution was stirred for 2 d at room temperature. The process of the addition of TPOS was repeated up to four times for controlled particle growth. The final molar composition was TEOS : TPOS : C_{16}TMABr : TEA : H_2O : TIPB = 0.1 : 0.9 : 0.24 : 0.11 : 520 : 0.3x. The samples are denoted as TIPB-x-as (x indicates the amount of TIPB: 0, 0.4, 1 or 2).

Removal of surfactants from mesostructured nanoparticles and fabrication of colloidal crystals

A sample of TIPB-x-as (50 mL) was transferred into a dialysis membrane tube composed of cellulose (molecular weight cutoff 12 000–14 000 Da) and was dialyzed for 24 h against a mixture (250 mL) of 2 M aqueous acetic acid and 2-propanol (1 : 1, v/v) to remove TEA, C_{16}CMABr and TIPB. This process was repeated five times. Next, the tube that contained the MSNs was immersed in deionized water to remove acetic acid and 2-propanol; this process was repeated four times. To increase the colloidal stability, Amberlite was immersed in the colloidal solution, and the solution was maintained at room temperature for 2 d. These samples are denoted as TIPB-x-DI, where "DI" means "deionized". Finally, colloidal crystals were obtained by drying TIPB-x-DI slowly at room temperature on a plastic boat. The samples were easily removed from the boat and crushed for characterization. This pulverization process is necessary to obtain SEM images of the samples. These samples are denoted as TIPB-x-crystals. Please note that TIPB-x-DI means a colloidal solution, and TIPB-x-crystals mean powder samples.

Characterization

Dynamic light scattering (DLS) measurements were conducted on a HORIBA nanopartica SZ-100-S instrument at 25 °C. Transmission electron microscopy (TEM) images were obtained on a JEOL JEM-2010 microscope operating at 200 kV. Scanning electron microscopy (SEM) images were obtained on a HITACHI S5500 electron microscope operating at 10 kV. The samples for TEM and SEM measurements were dropped and dried on a carbon-coated micro-grid (Okenshoji Co.). Mean particle sizes and standard deviations were obtained by measuring the sizes of 150 nanoparticles in the TEM images. Nitrogen gas adsorption–desorption measurements were performed with an Autosorb-1 instrument (Quantachrome Instruments) at −196 °C. Samples were preheated at 120 °C for 24 h under vacuum. The pore-size distributions were roughly evaluated using the BJH (Barrett–Joyner–Halenda) method. CHN analysis data were obtained using a Perkin-Elmer 2400 Series II instrument. Thermogravimetric (TG) curves were obtained on a RIGAKU Thermo Plus 2 instrument under a dry air flow at a heating rate of 10 °C min^{-1} up to 900 °C. ^{29}Si MAS NMR spectra were recorded on a JEOL JNM-CMX-400 spectrometer at a resonance frequency of 79.42 MHz with a 45° pulse. The recycle delay of the samples was 100 s. Chemical shifts for ^{29}Si NMR were referenced to polydimethylsilane at −33.8 ppm. Zeta-potential measurements were conducted with an Otsuka Electronics ELSZ-1 apparatus at 20 °C using the Smoluchowski equation to approximate the potential.

Results and discussion

Preparation of pore-expanded monodisperse colloidal MSNs

The particle size and its distribution as well as the dispersibility of pore-expanded monodisperse colloidal MSNs prepared with different amounts of the pore-expanding agent, TIPB, are shown in this section. In addition, we will discuss the effects of the amount of TIPB on the particle size distribution. Please note that there are only slight differences between TIPB-x-as and TIPB-x-DI in terms of the particle size, particle size distribution and mesostructure. The characterization results of TIPB-x-as are shown in the ESI (Fig. S1–S3†). The colloidal solution of TIPB-0-seed was nearly transparent in the visible light region, and no precipitates were observed. The hydrodynamic diameter of the nanoparticles was 50 nm and the mean diameter estimated from the TEM images was 40 nm (Fig. S4, ESI†). The standard deviation of the diameter was calculated to be 5.6 nm, which is the same as that in our previous report.[25]

All colloidal solutions of TIPB-x-DI were nearly transparent in the visible light region, and no precipitates were observed (Fig. S5, ESI†). All TIPB-x-DI had quite high colloidal stability because these MSNs had relatively high ζ potentials, and retained the colloidal state perfectly for a long time. The hydrodynamic diameter distributions calculated from DLS showed only one peak at ca. 100 nm (Fig. S6, ESI†). In addition, poly-dispersity indices were calculated to be less than 0.1 in all
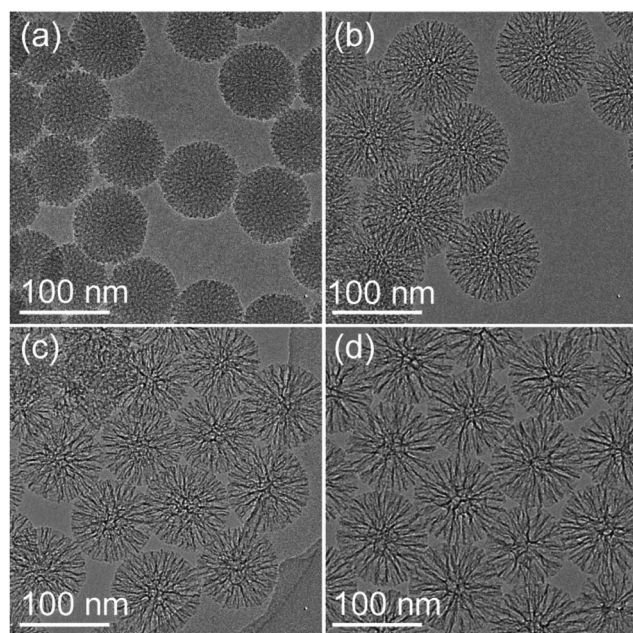
Fig. 1   TEM images of TIPB-x-DI ((a) $x = 0$, (b) $x = 0.4$, (c) $x = 1$ and (d) $x = 2$).

samples (*ca.* 0.05), which means these samples have a high monodispersity. The TEM images of TIPB-x-DI ($x = 0$, 0.4, 1 and 2) showed that the nanoparticles had uniform spherical shapes with mean diameters of 87 nm, 93 nm, 99 nm and 102 nm, respectively (Fig. 1). These indicate that the nanoparticles after seed growth were stably dispersed as primary nanoparticles. The relative standard deviations of the dia-

meters were calculated to be 6%, 5%, 7% and 9% for TIPB-x-DI ($x = 0$, 0.4, 1 and 2), respectively. Although the standard deviations slightly increased when large amounts of TIPB were added, these standard deviations were almost the same as that of TIPB-0-seed (Fig. S4, ESI†). These standard deviations indicate that these MSNs have monodispersity high enough to form colloidal crystals. In addition, the TEM images and SEM images showed that TIPB-x-DI ($x = 0$, 0.4) had mesopores of *ca.* 3 nm and 7 nm, respectively, and that TIPB-x-DI ($x = 1$, 2) had mesopores of ten plus several nm, which indicates that TIPB acted as a pore-expanding agent as expected (Fig. 2 and 3). From these results, we confirmed that monodisperse, pore-expanded MSNs were successfully obtained by adding TIPB during the growth of the seed nanoparticles. In addition, we succeeded in controlling both the particle and pore sizes of MSNs independently while retaining their monodispersity. The particle size of pore-expanded MSNs ($x = 0.4$, 1 or 2) was precisely controlled in the range of *ca.* 60–100 nm by changing the amount of TPOS added for the seed growth (please see the ESI for the experimental details and Fig. S7–S9 and Table S1†). The TEM images showed almost no change in the pore size when the amount of TIPB was constant. This remarkable pore and particle size controllability should be useful for various applications.

The presence of TIPB during the controlled growth only slightly affected the size distribution of the grown nanoparticles. In addition to the slow hydrolysis rate of TPOS, the stepwise addition of TPOS should lead to a low feed rate of hydrolysed silicate, which inhibits the generation of nuclei because the concentration of silicate in the seed solution remains low enough for almost all silicate to be used for the
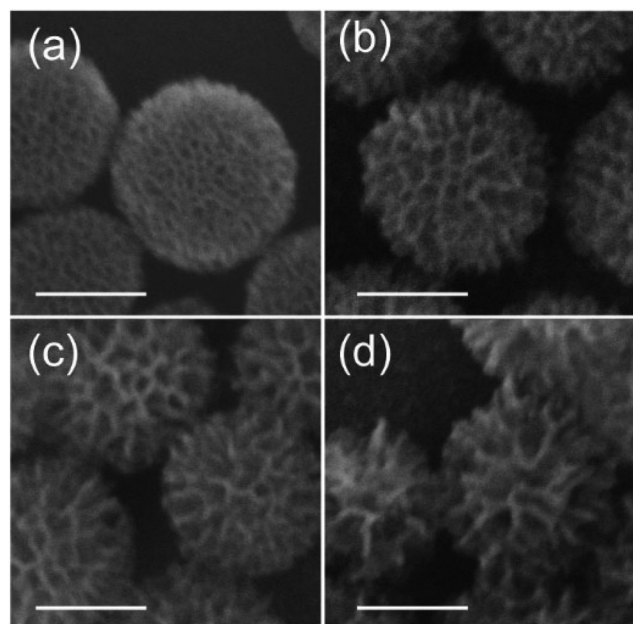

Fig. 2   SEM images of TIPB-x-DI ((a) $x = 0$, (b) $x = 0.4$, (c) $x = 1$, and (d) $x = 2$). Scale bar indicates 50 nm.
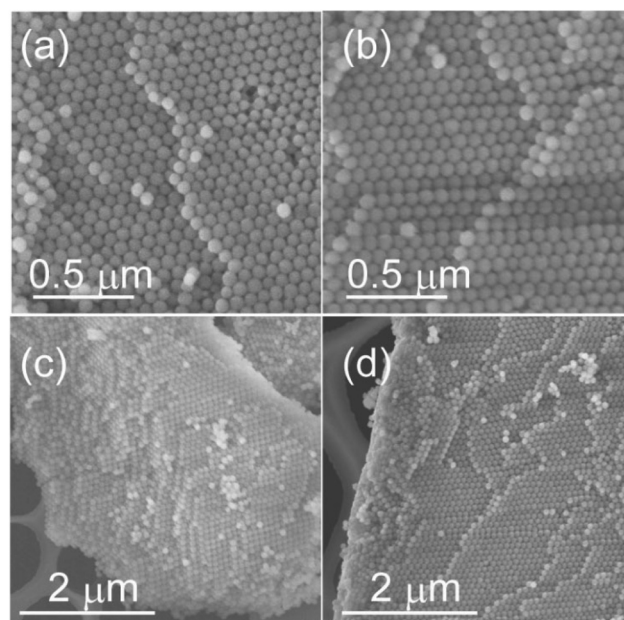

Fig. 3   SEM images of TIPB-x-crystals ((a) $x = 0$, (b) $x = 0.4$) and SEM images of TIPB-x-crystals with low magnification (c) $x = 0$, and (d) $x = 0.4$).
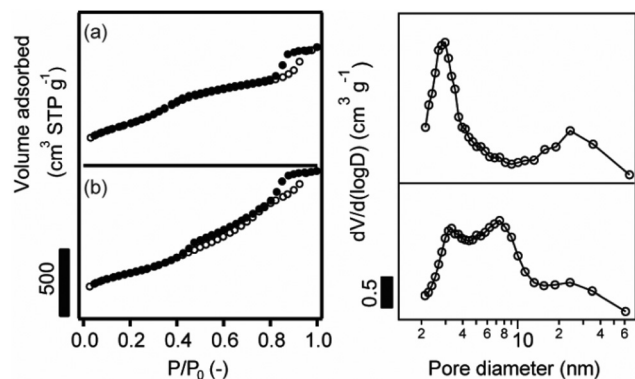
Fig. 4 N$_2$ adsorption and desorption isotherms (left) and pore size distributions (right) of TIPB-x-crystals ((a) x = 0, (b) x = 0.4).

growth. Therefore, this growth method allows the introduction of TIPB while retaining the monodispersity of the MSNs.

It should be noted that the pore-expanding agents should be added only during the growth process. The preparation of seed nanoparticles requires very strict conditions to obtain monodispersity. In fact, polydispersed MSNs were observed when TIPB was added during the preparation of the seed nanoparticles (please see the ESI for the experimental details and Fig. S10 and S11†).

Fabrication of colloidal crystals composed of pore-expanded MSNs

Colloidal crystals were prepared by drying TIPB-x-DI. Almost no existence of organic species was confirmed by CHN and TG analyses (Fig. S12 and Table S2, ESI†). The ordered arrays of nanoparticles were entirely observed in the SEM images of TIPB-x-crystals (x = 0, 0.4) (Fig. 3(a)–(d)). Unfortunately, TIPB-1-crystals and TIPB-2-crystals showed collapsed structures (Fig. S13(a) and (b), ESI†). Although TIPB-1-crystals have some spherical structures and their assembled structures, TIPB-2-crystals had only collapsed nanoparticles as discussed later (next section). N$_2$ adsorption–desorption measurements show that TIPB-0-crystals and TIPB-0.4-crystals have type IV isotherms according to the IUPAC classification (Fig. 4(a) and (b)). The pore size distribution of TIPB-0-crystals, calculated using the BJH method from the adsorption branch, shows a mesopore size of 3 nm and an interparticle pore size of 20 nm. TIPB-0.4-crystals show mesopores of 7 nm in size and interparticle pores of 20 nm in size, which indicates the successful expansion of the mesopores. In addition, mesopores 3 nm in size, derived from non-expanded mesopores, are observed. To the best of our knowledge, this is the first preparation of colloidal crystals with such large mesopores in their component nanoparticles. To evaluate the packing quality of the colloidal crystals, the neck sizes calculated from the N$_2$ desorption isotherms were compared with that of the ideal closest-packed colloidal crystals (eqn (S1), ESI†). The neck sizes of colloidal crystals were calculated by the desorption branch. The desorption branch of the isotherm with the hysteresis loops of Type

Table 1 Relationship between pore sizes and the formability of colloidal crystals

	TIPB-0	TIPB-0.4	TIPB-1	TIPB-2
Pore size	3 nm	3 nm 7 nm	10 nm	Ten and several nm
Formability of crystals	Formed	Formed	Almost collapsed	Completely collapsed

Pore size →
Mechanical stability →

H2 normally reflects the pore size of the most narrow place which is the neck of colloidal crystals in this case because the neck blocks the evaporation of nitrogen in the large sized pores.[55] The calculated neck sizes of TIPB-0-crystals and TIPB-0.4-crystals are 15 nm and 12 nm, respectively, while the ideal neck size is 14 nm. These results indicate that these colloidal crystals are almost entirely close-packed because the neck size is almost the same as the ideal calculated size. Unfortunately, the isotherms of TIPB-1-crystals and TIPB-2-crystals indicate that there are no clear pores (Fig. S13(a) and (b), ESI†). The disappearance of the pores strongly suggests the collapse of the nanoparticles, as discussed later. The relationship between pore sizes and the formability of colloidal crystals is summarized in Table 1. Such colloidal crystals composed of pore-expanded MSNs should be useful for various potential applications, such as unique templates and photonic crystals. Relatively large functional nanoparticles and photochemical substances, which have been limited to incorporation into mesopores, can be integrated to vary the functions of colloidal crystals. For example, the introduction of larger sized nanoparticles with magnetic or plasmonic properties into colloidal crystals should lead to the preparation of unique magneto-photonic crystals or plasmonic photonic crystals because the properties strongly depend on the size of nanoparticles.

Factors affecting the formation of colloidal crystals composed of pore-expanded MSNs

We succeeded in preparing colloidal crystals composed of pore-expanded MSNs, although TIPB-1-crystals and TIPB-2-crystals did not form ordered structures. In this section, we discuss the essential factors affecting the fabrication of colloidal crystals composed of pore-expanded MSNs on the basis of both their colloidal and mechanical stabilities.

In general, it is known that the formation of colloidal crystals requires sufficient colloidal stability and monodispersity. To arrange nanoparticles in order, the nanoparticles must retain their colloidal dispersity as primary nanoparticles in a solution with a particle volume fraction over 50%. The colloidal stability of silica nanoparticles strongly depends on the surface density of the silanol groups because they generate silanolate groups having a negative charge or solvation force.[56] We assume that the MSNs reported previously did not have sufficient amounts of silanol groups to form ordered colloidal

crystals. In fact, the MSNs reported by Zhao *et al.* had a small number of silanol groups ($Q^3/Q^4 = 0.4$).[44] In our case, the ^{29}Si MAS NMR spectra of TIPB-*x*-crystals show that all samples have $(2Q^2 + Q^3)/Q^4 = ca.$ 0.75 (Fig. S14, ESI†), which indicates that these nanoparticles have relatively large numbers of silanol groups. Due to the high density of silanol groups, the zeta potential values of these nanoparticles were *ca.* −25 mV, which should be sufficient to form colloidal crystals. Although the details still remain unclear, this structural difference should be derived from the preparative conditions of the nanoparticles. For example, we removed the templates through a dialysis process which does not involve drying processes. These factors probably lead to the high silanol density of MSNs in our case.

The mechanical stability of the colloidal crystals is also discussed by considering why the pores and morphology of TIPB-*x*-crystals collapsed. We succeeded in preparing ordered colloidal crystals in TIPB-0-crystals and TIPB-0.4-crystals, though TIPB-1-crystals and TIPB-2-crystals showed disordered and collapsed structures. Meanwhile, TIPB-1-DI and TIPB-2-DI retained their pore-expanded mesostructures and morphology during characterization (Fig. 2). Although the TIPB-*x*-DI samples were directly dropped on a TEM grid, the TIPB-*x*-crystal samples were dropped on a TEM grid after pulverization of their monoliths. This indicates that a decrease in the mechanical stability of the nanoparticles is responsible for this collapse of their structures and morphology. In fact, when the colloidal crystals prepared on a silicon substrate were directly observed by SEM without any pulverization process, assemblies of MSNs (TIPB-1-DI and TIPB-2-DI) with expanded mesopores were confirmed (Fig. S15, ESI†). Furthermore, the N$_2$ adsorption–desorption isotherm of TIPB-1-crystals without any heating or pulverization processes shows that the sample still contained mesopores (Fig. S16 (left), ESI†). The pore size of MSNs was calculated to be 9.6 nm (Fig. S17 (left), ESI†), which indicates that TIPB-1-crystals without any heating or pulverizing processes can retain their mesostructure and morphology. Unfortunately, TIPB-2-crystals collapsed even by just drying under vacuum conditions may be due to their extremely weak framework (Fig. S16 (right) and S17 (right), ESI†).

From these results, we found that a high density of silanol groups as well as the monodispersity of MSNs is important to form colloidal crystals, although MSNs with larger mesopores have lower mechanical stability. Therefore, it should be essential to increase the mechanical stability to prepare colloidal crystals composed of pore-expanded MSNs. For example, the increase in the wall thickness of the MSNs by an appropriate method, such as the addition of extra silica sources after the template removal process, might be effective.

Conclusion

MSNs with controlled pore and particle sizes were successfully prepared using a sophisticated growth method. This growth method allows the addition of pore-expanding agents while retaining the monodispersity of the MSNs. The pore and particle sizes can be easily controlled independently by changing the amounts of a pore-expanding agent and silica source, which expands the applicability of the growth method. Furthermore, colloidal crystals with large mesopores in their component nanoparticles were fabricated for the first time using these pore-expanded MSNs. For the fabrication of colloidal crystals composed of MSNs with expanded pores, tuning of the pore size is quite important because excessive expansion of the mesopores leads to the collapse of the structures. These large mesopores will enable us to introduce various useful guest species, such as biomolecules and metal nanoparticles, into the colloidal crystals. These composite colloidal crystals should be valuable in various applications, such as catalysts and devices.

Acknowledgements

Notes and references

1 A. Vu, X. Li, J. Phillips, A. Han, W. H. Smyrl, P. Bühlmann and A. Stein, *Chem. Mater.*, 2013, **25**, 4137.
2 L. Ye, Y. Wang, X. Chen, B. Yue, S. Chi Tsang and H. He, *Chem. Commun.*, 2011, **47**, 7389.
3 A. Stein and R. C. Schroden, *Curr. Opin. Solid State Mater. Sci.*, 2001, **5**, 553.
4 J. Han and V. Crespi, *Phys. Rev. Lett.*, 2001, **86**, 696.
5 Y. Xia, B. Gates, Y. Yin and Y. Lu, *Adv. Mater.*, 2000, **12**, 693.
6 O. D. Velev and A. M. Lenhoff, *Curr. Opin. Colloid Interface Sci.*, 2000, **5**, 56.
7 S. A. Johnson, *Science*, 1999, **283**, 963.
8 B. Gates, Y. Yin and Y. Xia, *Chem. Mater.*, 1999, **11**, 2827.
9 G. L. Egan, J. S. Yu, C. H. Kim, S. J. Lee, R. E. Schaak and T. E. Mallouk, *Adv. Mater.*, 2000, **12**, 1040.
10 S. Kang, J.-S. Yu, M. Kruk and M. Jaroniec, *Chem. Commun.*, 2002, 1670.
11 G. von Freymann, V. Kitaev, B. V. Lotsch and G. A. Ozin, *Chem. Soc. Rev.*, 2013, **42**, 2528.
12 J. Wang, Y. Zhang, S. Wang, Y. Song and L. Jiang, *Acc. Chem. Res.*, 2011, **44**, 405.
13 K. Lee and S. A. Asher, *J. Am. Chem. Soc.*, 2000, **122**, 9534.
14 R. Rengarajan, P. Jiang, V. Colvin and D. Mittleman, *Appl. Phys. Lett.*, 2000, **77**, 3517.
15 H. C. Zeng, *J. Mater. Chem.*, 2006, **16**, 649.
16 X. Xu and S. A. Asher, *J. Am. Chem. Soc.*, 2004, **126**, 7940.
17 Y. Wang, A. D. Price and F. Caruso, *J. Mater. Chem.*, 2009, **19**, 6451.

18 Y. A. Vlasov, K. Luterova, I. Pelant, B. Hönerlage and V. N. Astratov, *Appl. Phys. Lett.*, 1997, **71**, 1616.

19 K. Yoshino, S. B. Lee, S. Tatsuhara, Y. Kawagishi, M. Ozaki and A. A. Zakhidov, *Appl. Phys. Lett.*, 1998, **73**, 3506.

20 J. I. L. Chen, G. von Freymann, S. Y. Choi, V. Kitaev and G. A. Ozin, *Adv. Mater.*, 2006, **18**, 1915.

21 E. Yamamoto and K. Kuroda, *Bull. Chem. Soc. Jpn.*, 2016, **89**, 501.

22 E. Y. Trofimova, D. A. Kurdyukov, S. A. Yakovlev, D. A. Kirilenko, Y. A. Kukushkina, A. V. Nashchekin, A. A. Sitnikova, M. A. Yagovkina and V. G. Golubev, *Nanotechnology*, 2013, **24**, 155601.

23 Y. Yamada, T. Nakamura and K. Yano, *Langmuir*, 2008, **24**, 2779.

24 C.-N. Chen, H.-P. Lin, C.-P. Tsai and C.-Y. Tang, *Chem. Lett.*, 2004, **33**, 838.

25 E. Yamamoto, M. Kitahara, T. Tsumura and K. Kuroda, *Chem. Mater.*, 2014, **26**, 2927.

26 Y. Yamada, T. Nakamura, M. Ishi and K. Yano, *Langmuir*, 2006, **22**, 2444.

27 Y. Wang and F. Caruso, *Adv. Funct. Mater.*, 2004, **14**, 1012.

28 T. Nakamura, Y. Yamada and K. Yano, *J. Mater. Chem.*, 2007, **17**, 3726.

29 N. Tatsuda, T. Nakamura, D. Yamamoto, T. Yamazaki, T. Shimada, H. Inoue and K. Yano, *Chem. Mater.*, 2009, **21**, 5252.

30 T. Nakamura, Y. Yamada and K. Yano, *Microporous Mesoporous Mater.*, 2009, **117**, 478.

31 T. L. Kelly, Y. Yamada, C. Schneider, K. Yano and M. O. Wolf, *Adv. Funct. Mater.*, 2009, **19**, 3737.

32 G. L. Drisko, A. Carretero-Genevrier, A. Perrot, M. Gich, J. Gazquez, J. Rodriguez-Carvajal, L. Favre, D. Grosso, C. Boissiere and C. Sanchez, *Chem. Commun.*, 2015, **51**, 4164.

33 S. Murai, S. Yao, T. Nakamura, T. Kawamoto, K. Fujita, K. Yano and K. Tanaka, *Appl. Phys. Lett.*, 2012, **101**, 151121.

34 H. Yamada, T. Nakamura, Y. Yamada and K. Yano, *Adv. Mater.*, 2009, **21**, 4134.

35 L. Bai, Z. Xie, K. Cao, Y. Zhao, H. Xu, C. Zhu, Z. Mu, Q. Zhong and Z. Gu, *Nanoscale*, 2014, **6**, 5680.

36 T. Nakamura, Y. Yamada, H. Yamada and K. Yano, *J. Mater. Chem.*, 2009, **19**, 6699.

37 N. Z. Knezevic and J. O. Durand, *Nanoscale*, 2015, **7**, 2199.

38 X. Du and S. Z. Qiao, *Small*, 2015, **11**, 392.

39 H. Yamada, H. Ujiie, C. Urata, E. Yamamoto, Y. Yamauchi and K. Kuroda, *Nanoscale*, 2015, **7**, 19557.

40 M. Wu, Q. Meng, Y. Chen, Y. Du, L. Zhang, Y. Li, L. Zhang and J. Shi, *Adv. Mater.*, 2015, **27**, 215.

41 M. Mizutani, Y. Yamada, T. Nakamura and K. Yano, *Chem. Mater.*, 2008, **20**, 4777.

42 F. Gao, P. Botella, A. Corma, J. Blesa and L. Dong, *J. Phys. Chem. B*, 2009, **113**, 1796.

43 S. Gai, P. Yang, P. Ma, L. Wang, C. Li, M. Zhang and L. Jun, *Dalton Trans.*, 2012, **41**, 4511.

44 D. Shen, J. Yang, X. Li, L. Zhou, R. Zhang, W. Li, L. Chen, R. Wang, F. Zhang and D. Zhao, *Nano Lett.*, 2014, **14**, 923.

45 D. S. Moon and J. K. Lee, *Langmuir*, 2012, **28**, 12341.

46 A. B. D. Nandiyanto, S. G. Kim, F. Iskandar and K. Okuyama, *Microporous Mesoporous Mater.*, 2009, **120**, 447.

47 K. Zhang, L. L. Xu, J. G. Jiang, N. Calin, K. F. Lam, S. J. Zhang, H. H. Wu, G. D. Wu, B. Albela, L. Bonneviot and P. Wu, *J. Am. Chem. Soc.*, 2013, **135**, 2427.

48 D. Niu, Z. Liu, Y. Li, X. Luo, J. Zhang, J. Gong and J. Shi, *Adv. Mater.*, 2014, **26**, 4947.

49 Y. S. Lin, C. Y. Lu, Y. Hung and C. Y. Mou, *ChemPhysChem*, 2009, **10**, 2628.

50 V. Cauda, A. Schlossbauer, J. Kecht, A. Zürner and T. Bein, *J. Am. Chem. Soc.*, 2009, **131**, 11361.

51 T. Nakamura, M. Mizutani, H. Nozaki, N. Suzuki and K. Yano, *J. Phys. Chem. C*, 2006, **111**, 1093.

52 K. Yano and T. Nakamura, *Chem. Lett.*, 2006, **35**, 1014.

53 Y. S. Lin, C. P. Tsai, H. Y. Huang, C. T. Kuo, Y. Hung, D. M. Huang, Y. C. Chen and C. Y. Mou, *Chem. Mater.*, 2005, **17**, 4570.

54 H. Ishii, T. Ikuno, A. Shimojima and T. Okubo, *J. Colloid Interface Sci.*, 2015, **448**, 57.

55 M. Thommes, K. Kaneko, A. V. Neimark, J. P. Olivier, F. Rodriguez-Reinoso, J. Rouquerol and K. S. W. Sing, *Pure Appl. Chem.*, 2015, 87.

56 J. N. Israelachvili, *Intermolecular and Surface Forces*, Elsevier Inc., 3rd edn, 2011.